Rheologica Acta (2018) 57:645–653
https://doi.org/10.1007/s00397-018-1106-8

ORIGINAL CONTRIBUTION

Wall slip and multi-tier yielding in capillary suspensions

Amit Ahuja[1,2] · Tatyana Peifer[2] · Candice Claire Yang[2] · Omar Ahmad[2] · Chaiwut Gamonpilas[3]

Received: 21 April 2018 / Revised: 18 August 2018 / Accepted: 23 August 2018 / Published online: 8 September 2018

Abstract

Impact of wall slip on the yield stress measurement is examined for capillary suspensions consisting of cocoa powder as the dispersed phase, vegetable oil as the continuous primary fluid, and water as the secondary fluid using smooth and serrated parallel plates. Using dynamic oscillatory measurements, we investigated the yielding behavior of this ternary solid-fluid-fluid system with varying particle volume fraction, ϕ, from 0.45 to 0.65 and varying water volume fraction, ϕ_w, from 0.02 to 0.08. Yield stress is defined as the maximum in the elastic stress ($G'\gamma$), which is obtained by plotting the product of elastic modulus (G') and strain amplitude (γ) as a function of applied strain amplitude. With serrated plates, which offer minimal slippage, capillary suspensions with $\phi \geq 0.45$ and a fixed $\phi_w = 0.06$ showed a two-step yielding behavior as indicated by two peaks in the plots of elastic stress as a function of strain amplitude. On the other hand with smooth plates, the capillary suspensions showed strong evidence of wall slip as evident by the presence of three distinct peaks and lowered first yield stresses for all ϕ and ϕ_w. These results can be interpreted based on the fact that a particle-depleted layer, which is known to be responsible for slip, is present in the vicinity of the smooth surfaces. The slip layer presents itself as an additional "pseudo-microstructure" (characteristic length scale) besides the two microstructures, aqueous bridges and solid particle agglomerates, that may occur in the system. With serrated plates, both the yield stresses (σ_1, σ_2) and storage moduli plateau at lower strain (before the first yield point) and at higher strain (before the second yield point) (G'_{p1}, G'_{p2}) were found to increase with ϕ (at a fixed $\phi_w = 0.06$) following power-law dependences. Similarly with increasing ϕ_w (0.02 – 0.08) at a fixed $\phi = 0.62$, the system behaved as a solid-like material in a jammed state with particles strongly held together as manifested by rapidly increasing σ_1 and σ_2. The usage of smooth surfaces primarily affected σ_1 which was reflected by an approximately 70–90% decrement in the measured σ_1 for all values of ϕ. By contrast, σ_2 and G'_{p2} were found to be unaffected as shown by close agreement of values obtained using serrated geometry due to vanishing slip layers at higher strain amplitudes.

Keywords Capillary suspensions · Yield stress · Rheology · Wall slip · Cocoa particle · Viscoelasticity

Introduction

Investigating the influences of microstructure on the rheological properties of complex materials is vital for stability, quality assurance, consumer-perceived attributes and also to economically produce at manufacturing plants. An extensive array of structured materials of industrial importance like colloids, polymers, foams, micelles, gels, and emulsions display viscoelastic behaviors primarily attributed to the microscopic internal organization of the constituents leading to a networked structure. The bulk viscoelastic behavior is dictated by the characteristic microstructure of the particular system. Manufacturing and controlling viscoelastic materials with large viscosity and yield stress is a difficult industrial affair. For suspensions, the flow is controlled by the interactions among the particles such as hydrodynamic, Brownian, van der Waals, and repulsive

Electronic supplementary material The online version of this article (https://doi.org/10.1007/s00397-018-1106-8) contains supplementary material, which is available to authorized users.

✉ Amit Ahuja
amitahuja502@gmail.com

Chaiwut Gamonpilas
chaiwutg@mtec.or.th

[1] Benjamin Levich Institute and Department of Chemical Engineering, City College of City University of New York, 160 Convent Avenue, New York, NY, 10031, USA

[2] Cresilon Incorporation, 122 18th Street, Brooklyn, New York, NY, 11215, USA

[3] Polymer Physics Laboratory, National Metal and Materials Technology Center, 114 Thailand Science Park, Pahonyothin Road, Khlong Luang, Patumthani, 12120, Thailand

forces. Recently, the impact of capillary interactions and associated orders of magnitude changes in rheological properties in solid particle suspensions have attracted considerable attention in the literature (McCulfor et al. 2011; Koos and Willenbacher 2011; Koos et al. 2014; Koos 2014; Domenech and Velankar 2015; Bossler and Koos 2016; Yang and Velankar 2017). It has been demonstrated that by utilizing the capillary forces, rheological properties, stability against sedimentation, and textural attributes of materials can be fine tuned to a great extent to fulfill the requirements of formulation and processing (Hoffmann et al. 2014; Wollgarten et al. 2016). Apart from their potential usage in the formulation and processing of consumer goods, capillary forces have also been shown to play an important role in the rheology of hydrate slurries in the oil industry (Zylyftari et al. 2013; Ahuja et al. 2014, 2015; Ahuja 2015; Zylyftari et al. 2015; Karanjkar et al. 2016). Dispersing a small quantity of an immiscible liquid to a particle suspension can trigger particle aggregation as a consequence of capillary bridging between the particles. The state of bridges between the particles is controlled by capillary force and can be used to manipulate the rheological attributes of suspensions by adjusting the volume of secondary phase, particle size, and interfacial tension between the two fluids extensively (Koos et al. 2012).

Tailoring the flow behavior of solid-fluid-fluid system using capillary bridging approach has several potential industrial applications. Hoffmann et al. (2014) and Wollgarten et al. (2016) investigated two food model systems, where capillary bridging was utilized as a new formulation pathway for next generation low-fat food products. They studied the stability and rheology of two food model systems, namely, corn starch and cocoa particles with vegetable oil as the primary fluid and water as the secondary fluid. The formation of capillary bridges between the cocoa particles was shown to improve the heat stability, texture, and rheological properties of the model chocolate system. In our previous work (Ahuja and Gamonpilas 2017), we extended the works of Hoffmann et al. (2014) and Wollgarten et al. (2016) on cocoa particle-based capillary suspensions by investigating the effect of the ingredients of the ternary blend on the rheological behavior over a broad range of composition. We focussed on the yielding mechanism of solid-fluid-fluid systems with varying particle volume fraction (ϕ) from ϕ = 0.25 to 0.65. We noted an interesting two-step yielding process in the capillary suspensions. We examined this behavior in detail and suggested plausible mechanisms for the observed two-step yielding behavior. However, this two-step yielding behavior has been observed in a variety of other systems as well (Koumakis and Petekidis 2011; Zhou et al. 2014; Shao et al. 2013; Shukla et al. 2015; Segovia-Gutiérrez et al. 2012; Datta et al. 2011; Sentjabrskaja et al. 2013; Chan and Mohraz 2012; Zhang et al. 2016; Zhao et al. 2014). A prevalent feature among all the different systems, studied so far, displaying two-tier yielding behavior is thought to be due to the presence of two competing interaction forces at particulate level or two characteristic dimensions or relaxation time scales.

Particulate suspensions are particularly challenging compositions in which coupling between the yield stress and wall slip can often lead to erroneous results. In the case of dispersions, a conventional wisdom is that a particle-depleted thin layer of fluid (continuous phase) exists adjacent to the wall of the test geometry (Barnes 1995; Buscall et al. 1993; Ahuja and Singh 2009; Yang and Yu 2017). The appearance of two plateaus or shoulders in a plot of measured storage modulus (G') with applied strain amplitude (γ) in a dynamic oscillatory test is a distinctive feature and a classic signature of the existence of wall slippage in a typical system with significant yield stress. Walls et al. (2003) investigated the yielding behavior of colloidal gels containing hydrophobic silica, polyether, and lithium salts. They noted two plateaus in G' (or two maxima in elastic stress), which were associated to wall slippage (due to particle-depleted thin layer adjacent to the walls) and yielding of the colloidal gel. This simply suggests that particle depleted slip layer (which is of the orders of few microns depending on the size of the particles used in the system) can falsely present itself as a microstructure; thus, an additional apparent yield stress is recorded in the measurement. A direct outcome of this is that there is an apparent yield stress due to slippage at the walls at lower stress than the bulk yield stress leading to ambiguous conclusions. It should be noted here that slip could also develop or appear at high strain rate ranges after bulk yielding in the form of intermediate plateaus. The plateaus at intermediate deformation, as noted in some viscoelastic systems, originate from wall slip which causes a sudden sharp drop in the measured property then holds the value constant over a certain range of deformation (Sochi 2010).

In this work, we examined the impact of slippage on the measurement of yield stress in capillary suspensions using smooth and serrated surfaces. We present results obtained from oscillatory strain sweep experiments to demonstrate multi-tier yielding for capillary suspensions. This work aims to provide new insight and trends on the role of slippage on the yielding behavior of capillary suspensions. Particularly, using smooth and serrated parallel plates, we investigated the yielding behavior of a ternary solid-fluid-fluid system with varying particle volume fraction (ϕ) and varying water volume fraction (ϕ_w). The impact of wall slippage, in terms of degree of underestimation, using smooth surfaces, on the measured system properties including the first and the second yield stresses (σ_1, σ_2) and the first and the second storage moduli (G'_{p1}, G'_{p2}) for a broad range of ϕ (0.45 – 0.65) and ϕ_w (0.02 – 0.06) is thoroughly examined.

Materials and methods

The details on the ingredients used in the formulation of capillary suspensions can be found in Ahuja and Gamonpilas (2017). Briefly, cocoa powder (Hershey Company) was purchased from a local supermarket. The cocoa particles were unsweetened, non-alkalized, fat content of 1%, and polydispersed system with a Sauter mean diameter of $d_{3,2}$ = 16.1 μm. Food grade vegetable oil (100% soybean, Stop & Shop brand) with a viscosity of 45 mPa.s at 25°C and a density of 0.88 g/cm^3 was used. Deionized water was used from a Millipore QTM system. For sample preparation, cocoa particles were mixed into the oil using a mechanical mixer (IKA, Eurostar 60) at 500 rpm for 2 min. Subsequently, a known amount of water was mixed to the suspension at 1000 rpm for 5 min. Rheological measurements were carried out using a stress-controlled rotational rheometer (AR 2000ex, TA Instruments) equipped with either a pair of 40 mm diameter smooth or serrated parallel plates. The serrated plates have roughness $O(100)$ μm. All measurements were performed at a fixed temperature of 25 °C and at a gap height of 1.5 mm between the plates, unless stated otherwise.

Results

Figure 1a shows G′ plotted as a function of oscillatory stress amplitude (σ) at a frequency (f) of 1 Hz for a fixed ϕ = 0.62 and ϕ_w = 0.03 (based on total volume) using smooth and roughened plates. For both smooth and rough plates, at lower stress limits, G′ remains constant showing a linear viscoelastic regime. Above a critical stress, the sample begins to yield as indicated by a decrease in G′. In the case of roughened geometry, G′ continues to decrease and exhibits a small, second plateau at higher values of σ. When a second critical stress (σ) is attained, G′ decreases further and the whole curve clearly shows two distinct yield points indicating yielding through two mechanisms in agreement with our previous work (Ahuja and Gamonpilas 2017). In our previous work, we showed that for $\phi \geq 0.45$, there is a continuous, sample-spanning, tightly packed networked structure of cocoa particle agglomerates.

One of the most plausible mechanistic hypothesis proposed, to explain the observed two-step yielding behavior, was that on applying σ smaller than the first yield stress, the capillary bridges between the particle agglomerates will elongate though the agglomerates remain intact. With increasing amplitude of oscillatory stress (greater than yield stress), the capillary bridges begin to break apart and agglomerates are broken which imparts fluidity to the system. The networked structure subsequently fragments at the first yield stress, which results in large agglomerates in a fluidized state. Within this fluidized state, individual particles remain jammed due to liquid capillary bridges between the particles. When the amplitude of applied oscillatory stress exceeds the second yield stress, the capillary bridges rupture and the clusters break further into smaller fragments, thus leading to complete yielding of the material. The presence of these two microstructures in the system leads to yielding in two stages.

Despite the similar behavior at lower values of σ, dependences of the sample moduli on the stress are distinctly related to the surface characteristics of the chosen geometry.

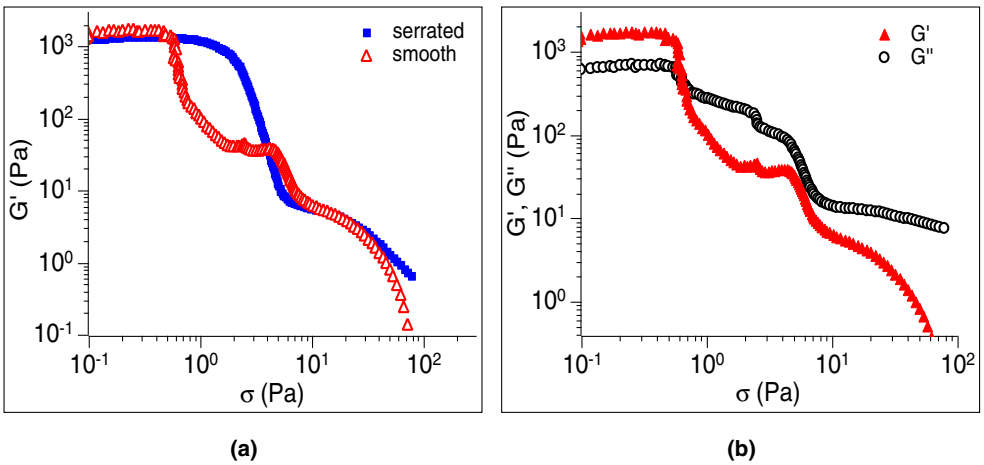

(a) (b)

Fig. 1 **a** Behavior of G′ is plotted as a function of σ in an oscillation amplitude sweep experiment carried out at f = 1 Hz on cocoa suspensions with a fixed ϕ = 0.62 and ϕ_w = 0.03 using smooth and serrated plates at a gap of 1.5 mm. **b** The behavior of both G′ and G″ for the same capillary suspension using smooth plates

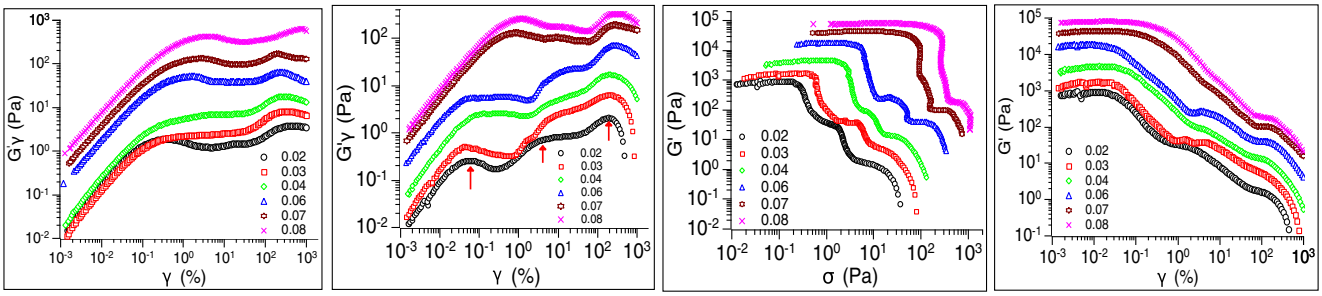

Fig. 2 **a** Elastic stress, $G'\gamma$, as a function of γ for cocoa suspensions with a fixed ϕ = 0.62 and varying ϕ_w (shown in legend) using serrated plates at a gap of 1.5 mm. **b** Same conditions and composition as **a** but using smooth plates. **c** G′ versus measured σ at the same conditions and composition as **b** using smooth plates. **d** Behavior of G′ is plotted as a function of γ at the same conditions and composition as for **b** using smooth plates. The data shown in **b**, **c**, and **d** are from the same tests but plotted differently to highlight the presence of three peaks/humps/plateaus

In the case of smooth geometry, the capillary suspensions displayed an additional plateau in comparison to rough ones, with three distinct plateaus in total when the result is plotted in terms of G′ versus σ. Anomaly of the moduli measured using smooth plates from those using rough plates begins to appear at lower stress and grows as intermediate levels of stress are approached, and is attributed to the wall slip due to the difference in the boundary condition. These results can be understood based on the fact that the particle-depleted layer, which is known to be responsible for slip, is present adjacent to both the smooth surfaces and these slip layers present themselves as an additional characteristic length scale besides two above-mentioned microstructures (aqueous bridges and solid particle agglomerates) present in the system. Furthermore, the deviations between the smooth geometry and the rough ones disappear at sufficiently higher amplitude of σ indicating the negligible effects of wall slip. Figure 1b shows the behavior of G′ and G″ for the case of smooth plates. G′ is larger than G″ at low stress amplitude ranges and G″ also shows three plateaus similar to G′.

In Fig. 2a, we show the elastic stress, $G'\gamma$, as a function of applied γ for cocoa suspensions with a fixed ϕ = 0.62 and varying ϕ_w (shown in legend) using serrated plates by simply recasting the data from oscillatory strain amplitude sweeps. In this plot, the two yield points can be seen more clearly displaying two yielding mechanisms in action, where the elastic stress shows two peaks for all ϕ_w considered here. Similar data is obtained using smooth plates and is shown in Fig. 2b. In this case, clearly, there are three distinct peaks due to slippage at the smooth boundaries. This behavior can also be observed when recasting the data by plotting G′ versus measured σ or applied γ for smooth plates as shown in Fig. 2c, d, respectively. Three distinctive plateaus for smooth plates in comparison to two plateaus for rough plates clearly demonstrate the presence of slippage when measuring with the smooth geometry for the whole range of ϕ_w explored in this study. Figure 3a–d shows the parameters obtained from Fig. 2a–b, namely, first and second yield stresses (σ_1, σ_2) and first and second plateau storage moduli (G'_{p1}, G'_{p2}) as a function of ϕ_w for a fixed ϕ = 0.62 for serrated and smooth geometries. Clearly, with increasing ϕ_w (0.02–0.08), all the four measured parameters increase exponentially. The only parameter which seems to be

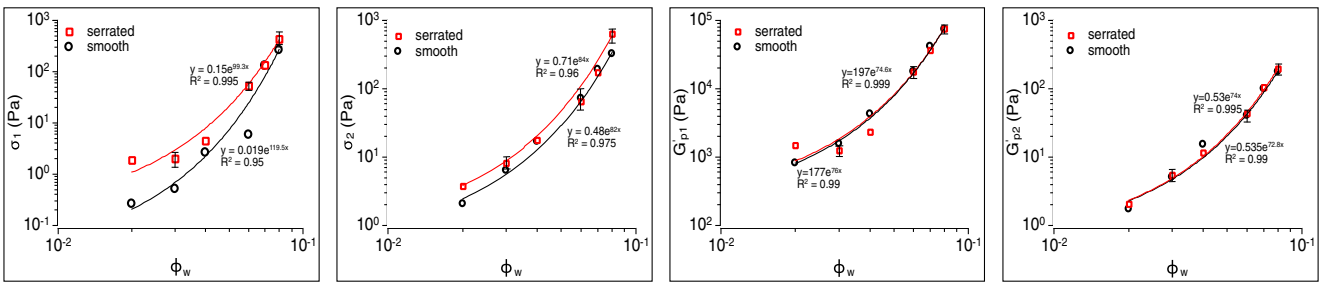

Fig. 3 **a** First yield stress (σ_1), taken as the maxima in elastic stress from Fig. 2a, b, as a function of ϕ_w for a fixed ϕ = 0.62 for serrated and smooth geometries. Similarly, a comparison of **b** second yield stress (σ_2), **c** first plateau storage modulus (G'_{p1}), and **d** second plateau storage modulus (G'_{p2}) is shown as a function of ϕ_w for a fixed ϕ = 0.62 for serrated and smooth geometries

affected the most due to slippage is σ_1 as can be seen by comparing the data obtained using serrated and smooth geometries in Fig. 3a. The other parameters obtained using serrated and smooth geometries are statistically comparable. As explained earlier, the discrepancy between the smooth geometry and the rough one vanishes at sufficiently higher amplitude of γ where the slip layers presumably get disintegrated completely, leading to similar values of σ_2 and G'_{p2} obtained from both geometries. At lower values of ϕ_w, the discrepancy in the measured σ_1 from the two geometries is large and this difference becomes negligible for suspensions with higher values of ϕ_w. In other words, the slippage is dominant for weak capillary suspensions formulated with lower amounts of aqueous phase while with higher amounts of aqueous phase, the capillary suspension becomes a paste-like material which exhibits weaker or negligible slippage at the walls.

Figure 4a–b shows the effect of ϕ (shown in legend) on the elastic stress ($G'\gamma$) as a function of γ for cocoa suspensions with a fixed ϕ_w (0.06) using serrated and smooth geometries. For serrated plates, two yield peaks are observed for all values of ϕ considered in this study. For smooth plates, three peaks or humps indicating the presence of slip layer at the smooth boundaries. Figure 4c shows the difference between the measured storage modulus, $\Delta G'$, from the two geometries as a function of applied γ for a fixed ϕ_w (0.06) and varying ϕ (shown in legend). Interestingly, $\Delta G'$ is relatively small at lower strain amplitudes for all values of ϕ with serrated geometry showing a somewhat higher value of G' than the smooth geometry. $\Delta G'$ increases with increasing strain amplitude and goes through a maximum at intermediate strain amplitudes for all values of ϕ. After reaching a maximum, $\Delta G'$ begins to decrease with increasing strain amplitudes and it eventually becomes zero at higher strain amplitudes as explained earlier due to vanishing slip layers at such higher strain amplitudes. The maxima difference, $\Delta G'_{max}$, due to slippage in the measured storage modulus from two geometries as a function of ϕ is plotted in Fig. 4d. As one can see, $\Delta G'_{max}$ increases with ϕ following a power-law and the correlation between the two is strong. Furthermore, the impact of wall slip on the measured properties using serrated and smooth plates as a function of ϕ and at a fixed ϕ_w is shown in Fig. 5a–e. The yield stresses and storage moduli increase with increasing ϕ following power-law dependences. As shown in Fig. 5a, the first yield stress measured using serrated plates is significantly higher than the yield stress obtained using smooth plates (see Figs. S1 and S2 in supplementary information for reproducibility). Figure 5b shows the degree of underestimation in the measurement of σ_1 as a function of ϕ from smooth geometry in comparison to the serrated geometry. The smooth geometry leads to an underestimation of σ_1 by approximately 70–90% in the whole range of ϕ covered in this work. There is no correlation between % underestimation of σ_1 and ϕ as opposed to $\Delta G'_{max}$ and ϕ as a measure of wall slip, shown previously in Fig. 4d. In contrast, the difference in other measured properties, shown in Fig. 5c–e, obtained using the two geometries are not statistically significant.

Apparent wall slip is induced by the development of a thin layer of the continuous phase at the solid boundaries. This lower-viscosity depleted zone acts as a lubricating regime, aiding the system to flow more readily. The use of different gap heights to detect the presence of wall slippage and also to perform mathematical corrections to the rheometric data is a common strategy to deal with and circumvent slippage. Figure 6a–c shows the dependence of gap on the measurements using serrated and smooth geometries. Figure 6a shows the elastic stress versus γ for cocoa suspensions with a fixed ϕ = 0.65 and ϕ_w = 0.06 using serrated geometry at different gaps. The measured elastic stress obtained at three different gaps superimposed on each other quite well indicating no dependence of the measurements on gaps between the plates thus no slippage at the walls. On the other hand, the elastic stress obtained

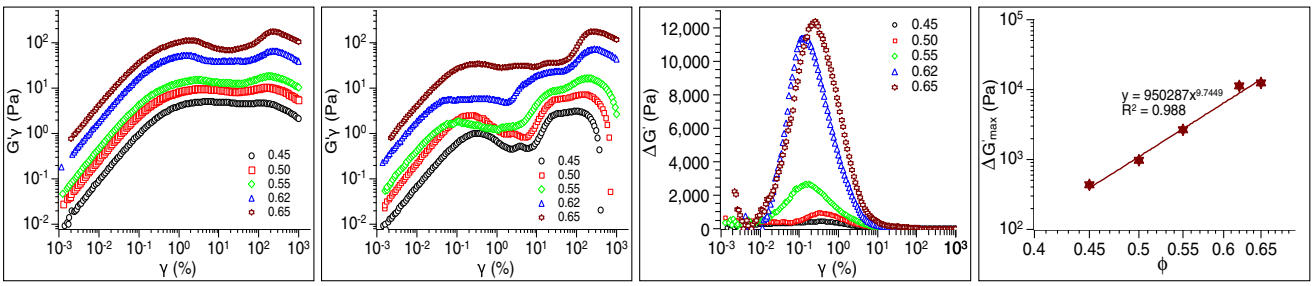

Fig. 4 **a** Elastic stress, $G'\gamma$, as a function of γ for cocoa suspensions with a fixed $\phi_w = 0.06$ and varying ϕ (shown in legend) using serrated plates at a gap of 1.5 mm. **b** Same conditions and composition as **a** but using smooth plates. **c** The difference between the measured storage modulus as a function of applied strain amplitude using serrated and smooth geometries for the same data as shown in **a** and **b**. **d** The maxima difference due to slippage in the measured storage modulus from two geometries (from **c**) as a function of ϕ

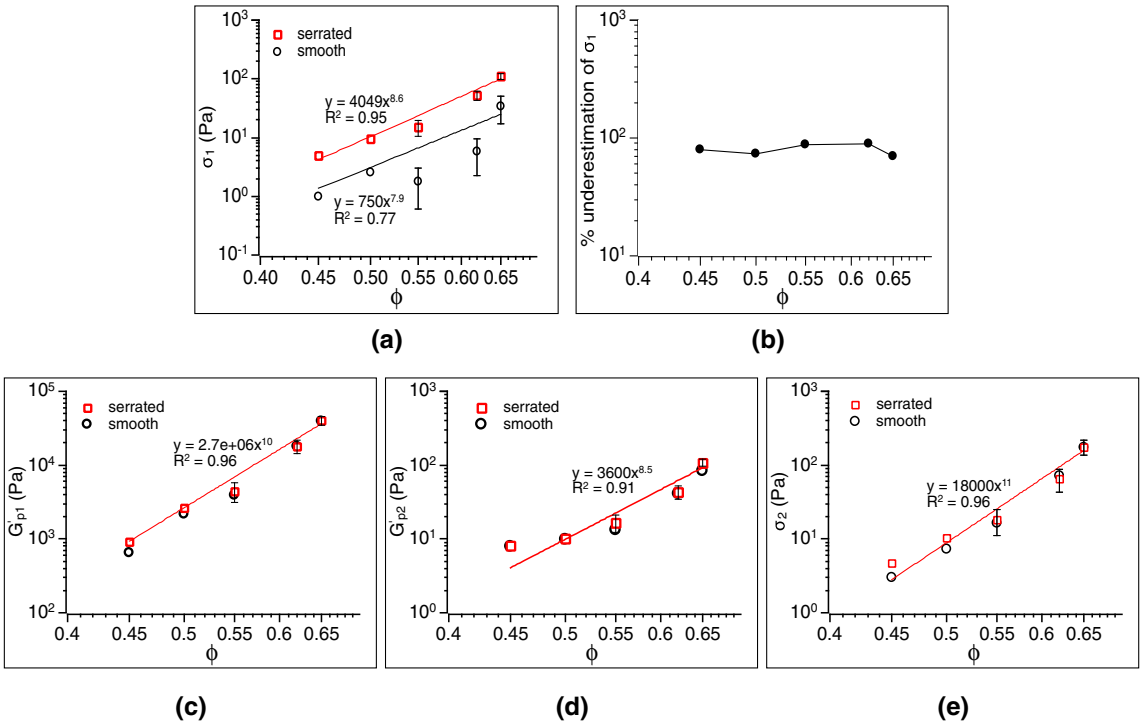

Fig. 5 **a** First yield stress (σ_1), taken as the maxima in elastic stress from Fig. 4a, b, as a function of ϕ for a fixed $\phi_w = 0.06$ for serrated and smooth geometries, **b** degree of underestimation for the measured σ_1 using smooth geometry in comparison to serrated geometry. A comparison of **c** first plateau storage modulus (G'_{p1}), **d** second plateau storage modulus (G'_{p2}), and **e** second yield stress (σ_2) are shown as a function of ϕ for a fixed $\phi_w = 0.06$ for serrated and smooth geometries

at two gaps differ significantly for the smooth plates; the one measured at a gap of 0.5 mm runs below the elastic stress curve measured at the gap of 2.5 mm. Moreover, at a gap of 0.5 mm, a broad plateau-like shoulder followed by two peaks are noted, while at a gap of 2.5 mm, four peaks (indicated by arrows) are observed. This behavior can be seen more clearly in Fig. 6c. The measured G′ is plotted as a function of measured σ at different gaps heights. Interestingly, for gap heights between 0.5–1.5 mm, only three plateaus were observed while with larger gap size ($\geq$ 2mm), four step-like plateaus were noted presumably due to two slip layers at both the upper and lower smooth surfaces. Note that in the parallel plate set up (for both smooth and serrated plates) utilized in this work, the bottom plate is stationary and the upper plate is rotatable. In order to understand if the development and growth of the slip

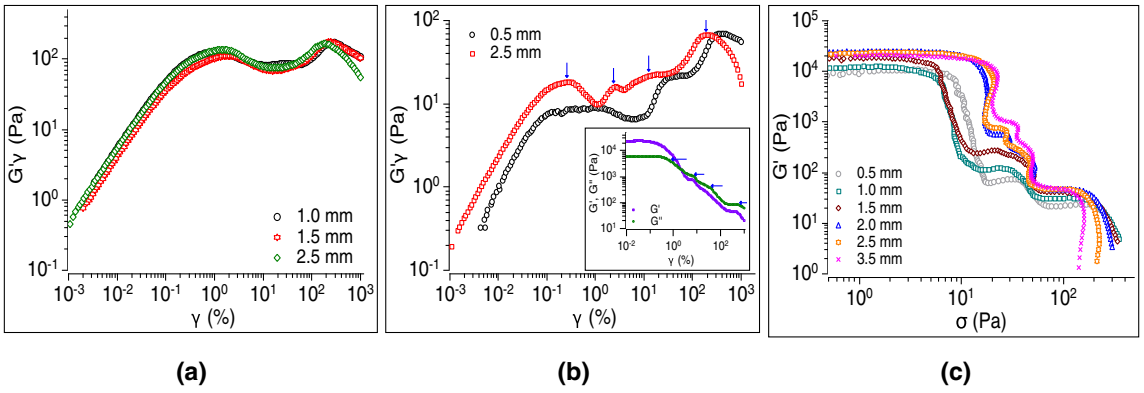

Fig. 6 **a** Elastic stress, G′γ, as a function of γ for cocoa suspensions with a fixed $\phi = 0.65$ and $\phi_w = 0.06$ using serrated geometry at different gaps between the plates (shown in legend). **b** Elastic stress as a function of γ for cocoa suspensions with a fixed $\phi = 0.62$ and $\phi_w = 0.06$ obtained using smooth geometry at gaps of 0.5 and 2.5 mm between the plates. The inset shows G′ and G″ behavior for the case of 2.5 mm gap between the plates. **c** The behavior of G′ versus measured σ for a fixed $\phi = 0.62$ and $\phi_w = 0.06$ using smooth plates at different gaps between the plates

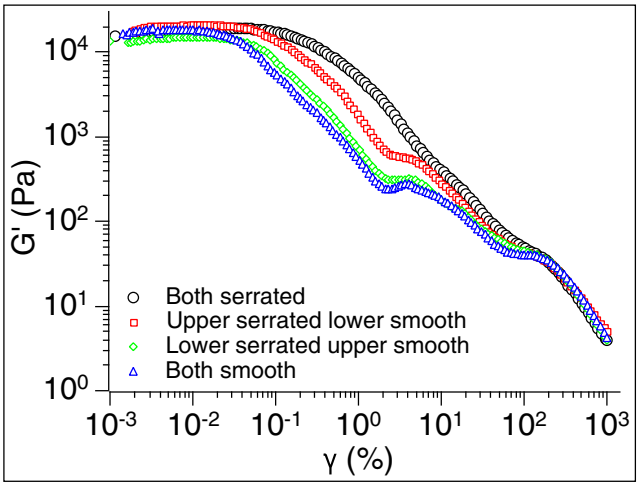

Fig. 7 G' as a function of applied γ at a frequency of 1 Hz and a gap of 1.5 mm between plates using different combination of smooth and serrated plates

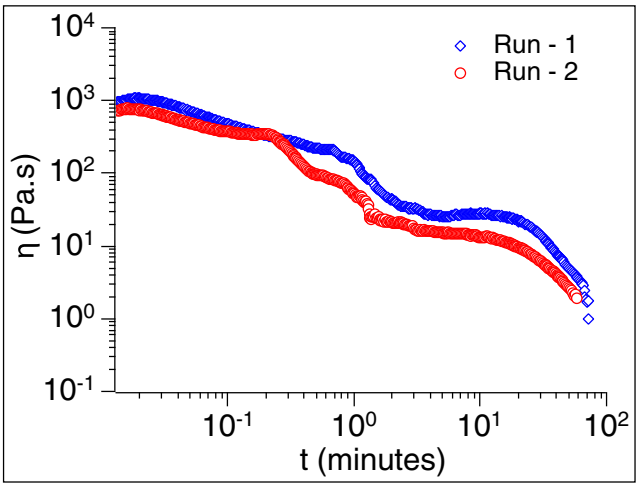

Fig. 8 Two replicates of creep experiment on a capillary suspension with $\phi = 0.62$ and $\phi_w = 0.06$ using a smooth geometry. The applied shear stress is 200 Pa. The plot shows viscosity response with time demonstrating the complexities of the yielding process in the presence of slippage

layer is promoted at a stationary or rotating plate, we performed experiments where two combinations of serrated and smooth plates were used as upper and lower attachments and the results are shown in Fig. 7. From this plot, one can see that having upper attachment (rotatable) smooth and lower attachment as serrated gives the same response in terms of the measured G' as with both smooth plates. On the other hand, having upper serrated attachment and lower smooth attachment suppress slippage to some extent but not completely; an intermediate plateau is noted with this combination as well. This suggests that the apparent slip layer grows to a greater degree adjacent to a rotating, smooth plate presumably due to the fact that particles or particle aggregates are pushed away from the moving plate towards the stationary plate which leads to a particle-lean layer of oil in the vicinity of the moving plate.

The presence of slippage and associated complexities of the yielding process are further corroborated by an additional creep test performed on a capillary suspension. A similar three-step yielding process was noted in the creep test as well, which distinctly showed the presence of two structures and slip layer at the walls. In Fig. 8, the fluidization of a capillary suspension under an applied shear stress (τ) in a typical creep experiment is shown to exhibit a complex multi-tier yielding process in terms of measured viscosity (η) response using a smooth geometry. This type of behavior has been observed in attractive gels made of carbon black particles in mineral oil by Grenard et al. (2014). One can clearly see that during the first step, η decreases significantly which is presumably due to rupturing of aqueous capillary bridges between the large aggregates, which is followed by a second drop in η which is due to slippage. Subsequently with increase in time, η decreases further in the last step, which is due to break down of the fluidized aggregates into smaller flocs. The purpose of this article was not to investigate the creep flow of capillary suspensions under applied shear stresses, though this experiment is chosen to include in the present work to demonstrate the complexities involved in the yielding process of this material using smooth boundary conditions. A detailed paper on associated timescale in creep and yielding of capillary suspensions will be published elsewhere separately.

Discussion

It is well established that a wall slip layer exists on smooth boundaries in the flow experiments of complex materials like polymer melts, suspensions, gels, emulsions, and pastes. A significant amount of work has been performed to provide a quantitative and mechanistic understanding of wall slip in the context of above-mentioned materials by direct or indirect methods (Kalyon 2005; Buscall et al. 1993; Yoshimura and Prud'Homme 1988; Ahuja and Singh 2009; Barnes 1995; Walls et al. 2003). In this work, we investigated how the boundary conditions affect the yielding behavior of a capillary suspension under large amplitude dynamic oscillatory sweep tests. A systematic experimental design with a capillary suspension system consisting of cocoa particles in oil as a primary fluid with a small volume of water as a secondary fluid was executed to explore the yielding dynamics of capillary suspensions in detail. Figure 1a shows an oscillation amplitude sweep response of cocoa suspension for a fixed $\phi = 0.62$ and $\phi_w = 0.03$ by employing smooth and roughened parallel plates. Both

geometries approximately give the same measure of G′ at low σ. However, in the case of smooth boundaries, slip begins to arise from low-to-moderate amplitudes of σ, which is noted as a divergence from the linear viscoelastic zone. At the onset of slippage and subsequent apparent yielding, an intermediate plateau or hump appears. At stress amplitudes corresponding to the intermediate G′ plateau, we expose the material adjacent to the wall with partially ruptured or yielded microstructure than the bulk. Under this scenario, wall slippage is prevalent despite some degree of yielding or partial microstructural failure.

To sum up the proposed hypothesis for the presence of the second plateau in G′ versus σ, wall slip appears presumably because of a particle-depleted, thin film-like layer of continuous oil phase in the vicinity of smooth walls deforming more than the rest of the bulk material. At moderately higher amplitudes of σ, typically post the second G′ plateau, the fluidized agglomerates of cocoa particles begin to break down further into smaller fragment and the bulk material starts to flow. The difference between the smooth plates and the rough ones disappears at adequately higher amplitude of σ where the impact of slippage is minimal. Presumably, this is due to the fact that the slip layers disintegrate completely at higher amplitudes leading to similar values of G′ from serrated and smooth geometries. The observations that both geometries give overlapping measure of G′ at lower and higher amplitudes of σ and the appearance of an additional intermediate plateau for the smooth geometry, suggest that there are primary and secondary structures along with wall slippage. The effect of water content on slip and yield stress is also examined in Fig. 2. It shows an elastic stress as a function of increasing γ for a fixed $\phi = 0.62$ using smooth and serrated plates. We noted that the modulus increases dramatically with ϕ_w and all samples display three G′ plateaus, indicative of the existence of slippage. The trends observed in our study may also be due to presence of shear bands, which make rheological measurements difficult to understand. This phenomenon is described as local regions in a sample where there is a discontinuity in the shear rate locally, when a globally applied shear rate is not transmitted homogeneously throughout the material. This behavior has been observed in many materials like suspensions, polymers, and gels (Divoux et al. 2016).

Since the capillary suspension modulus is a strong function of the cocoa particle volume fraction, oscillatory amplitude sweep experiments were performed as a function of the cocoa particle fraction for a fixed volume fraction of the aqueous phase using a smooth geometry. The presence of wall slippage is noted in all cases. The addition of cocoa particles increases the storage modulus and the yield stress. The degree of wall slippage measured as percentage underestimation in the first yield stress was found to be approximately 70–90% by changes in modulus obtained by adding more cocoa particles in the suspensions. This observation is consistent with the work of Walls et al. (2003) which showed approximately 62% underestimation in the measured yield stress due to wall slip for all the fumed silica concentrations used in their study to prepare the colloidal gels. However, on taking the difference between the measured storage moduli from serrated and smooth geometries and plotting the difference as a function of strain amplitude, we noted an interesting bell-shaped curve for all ϕ, where the difference in storage moduli attains a peak at intermediate deformations before becoming zero at higher deformations. The maxima in G′ difference was found to be a strong function of the increasing cocoa particle volume fraction following a power-law model indicating an increasing influence of wall slip on the measurements at higher cocoa particles fractions.

Conclusion

In this study, we measured yield stress of capillary suspensions composed of vegetable oil, cocoa particles and a small quantity of aqueous phase using oscillatory amplitude sweep experiments. The measurements in terms of elastic stress with serrated plates showed two peaks, representing two yield stresses thus two structures in the system. With serrated plates, capillary suspensions with $\phi \geq 0.45$ and a fixed $\phi_w = 0.06$ as the secondary fluid showed a two-tier yielding behavior as indicated by two plateaus in the plots of G′ as a function of γ. On the contrary with smooth surfaces, the capillary suspensions exhibited strong signatures of wall slip as identified by the presence of three or four distinct plateaus in the plots of G′ versus γ. The smooth geometries showed much lower first yield stress and an additional plateau appeared in the storage modulus versus strain amplitude plots. At higher strain amplitudes, the data on G′ versus γ plots of both smooth and roughened geometries converged. The use of smooth geometry mainly affected the first yield stress which was revealed by an approximately 70–90% decrement as compared to those measured by the serrated geometry for all values of ϕ. However, the second yield stress and both the plateau moduli were not affected significantly by the wall slippage as indicated by almost overlapping measures of these properties by smooth and serrated geometries. The large extent of wall slippage at the intermediate strain is also confirmed by the difference between the measured G′ using the two geometries plotted as a function of applied strain amplitude which begins with a small difference at lower deformations and grows to a maxima at intermediate levels of deformations and finally drops to zero at higher deformations due to vanishing slip layers at higher strain

amplitudes. The maximum in G′ difference increases with increasing ϕ following a power-law relationship indicating an increasing impact of wall slippage on the measurements at higher particle volume fractions. The yield stresses and plateau storage moduli were found to scale with power-law functions with increasing ϕ at a fixed ϕ_w. Similarly with increasing ϕ_w and at fixed ϕ, the system shifted to a compact state with agglomerates strongly held together as manifested by rapidly increasing first and second yield stresses.

Acknowledgements The authors are thankful to Professor Jeffrey Morris for numerous useful discussions and suggestions on improving the manuscript. The authors appreciate discussions with Megha Goyal regarding material selection, data processing, and plotting.

References

Ahuja A (2015) Hydrate forming emulsion: rheology and morphology analysis for flow assurance. PhD Thesis, City University of New York

Ahuja A, Gamonpilas C (2017) Dual yielding in capillary suspensions. Rheol Acta 56:10, 801

Ahuja A, Singh A (2009) Slip velocity of concentrated suspensions in Couette flow. J Rheol 53:6

Ahuja A, Zylyftari G, Morris JF (2014) Calorimetric and rheological studies on cyclopentane hydrate-forming water-in-kerosene emulsions. J Chem & Eng Data 60:362

Ahuja A, Zylyftari G, Morris JF (2015) Yield stress measurements of cyclopentane hydrate slurry. J Non–Newtonian Fluid Mech 220:116

Barnes HA (1995) A review of the slip (wall depletion) of polymer solutions, emulsions, and particle suspensions in viscometers: its cause, character, and cure. J Non-Newtonian Fluid Mech 56:221

Bossler F, Koos E (2016) Structure of particle networks in capillary suspensions with wetting and nonwetting fluids. Langmuir 32:1489

Bossler F, Weyrauch L, Schmidt R, Koos E (2017) Influence of mixing conditions on the rheological properties and structure of capillary suspensions. Colloids Surf A Physicochem Eng Asp 518:85–97

Buscall R, McGowan JI, Morton-Jones AJ (1993) The rheology of concentrated dispersions of weakly attracting colloidal particles with and without wall slip. J Rheol 37:621

Chan HK, Mohraz A (2012) Two-step yielding and directional strain-induced strengthening in dilute colloidal gels. Phys Rev E 85:041403

Datta SS, Gerrard DD, Rhodes TS, Mason TG, Weitz DA (2011) Rheology of attractive emulsions. Phys Rev E 84:041404

Divoux T, Fardin MA, Manneville S, Lerouge S (2016) Shear banding of complex fluids. Annu Rev Fluid Mech 48:81–103

Domenech T, Velankar SS (2015) On the rheology of pendular gels and morphological developments in paste-like ternary systems based on capillary attraction. Soft Matter 11:1500

Grenard V, Divoux T, Taberlet N, Manneville S (2014) Timescales in creep and yielding of attractive gels. Soft Matter 10:1555

Hoffmann S, Koos E, Willenbacher N (2014) Using capillary bridges to tune stability and flow behavior of food suspensions. Food Hydrocoll 40:44

Kalyon DM (2005) Apparent slip and viscoplasticity of concentrated suspensions. J Rheol 49:621

Karanjkar PU, Ahuja A, Zylyftari G, Lee JW, Morris JF (2016) Rheology of cyclopentane hydrate slurry in a model oil-continuous emulsion. Rheol Acta 55:235

Koos E (2014) Capillary suspensions: Particle networks formed through the capillary force. Curr Opin Colloid Interface Sci 19:575

Koos E, Willenbacher N (2011) Capillary forces in suspension rheology. Science 331:897

Koos E, Johannsmeier J, Schwebler L, Wiillenbacher N (2012) Tuning suspension rheology using capillary forces. Soft Matter 8:6620

Koos E, Kannowade W, Willenbacher N (2014) Restructuring and aging in a capillary suspension. Rheol Acta 53:947

Koumakis N, Petekidis G (2011) Two step yielding in attractive colloids: transition from gels to attractive glasses. Soft Matter 7:2456

McCulfor J, Himes P, Anklam MR (2011) The effects of capillary forces on the flow properties of glass particle suspensions in mineral oil. AIChE J 57:2334

Segovia-Gutiérrez JP, Berli CLA, de Vicente J (2012) Nonlinear viscoelasticity and two-step yielding in magnetorheology: a colloidal gel approach to understand the effect of particle concentration. J Rheol 56:1429

Sentjabrskaja T, Babaliari E, Hendricks J, Laurati M, Petekidis G, Egelhaaf SU (2013) Yielding of binary colloidal glasses. Soft Matter 9:4524

Shao Z, Negi AS, Osuji CO (2013) Role of interparticle attraction in the yielding response of microgel suspensions. Soft Matter 9:5492

Shukla A, Arnipally S, Dagaonkar M, Joshi YM (2015) Two-step yielding in surfactant suspension pastes. Rheol Acta 54:353–364

Sochi T (2010) Flow of non-Newtonian fluids in porous media. J Polym Sci B 48:2437

Walls HJ, Caines SB, Sanchez AM, Khan SA (2003) Yield stress and wall slip phenomena in colloidal silica gels. J Rheol 47(4):847

Wollgarten S, Yuce C, Koos E, Willenbacher N (2016) Tailoring flow behavior and texture of water based cocoa suspensions. Food Hydrocoll 52:167

Yang K, Yu W (2017) Dynamic wall slip behavior of yield stress fluids under large amplitude oscillatory shear. J Rheol 61:627

Yang J, Velankar SS (2017) Preparation and yielding behavior of pendular network suspensions. J Rheol 61:217

Yoshimura A, Prud'Homme RK (1988) Wall slip corrections for couette and parallel disk viscometers. J Rheol 32:53

Zhang H, Yu K, Cayre OJ, Harbottle D (2016) Interfacial particle dynamics: one and two step yielding in colloidal glass. Langmuir 32:13472

Zhao C, Yuan G, Han JCC (2014) Bridging and caging in mixed suspensions of microsphere and adsorptive microgel. Soft Matter 10:8905

Zhou Z, Hollingsworth JV, Hong S, Cheng H, Han CC (2014) Yielding behavior in colloidal glasses: Comparison between hard cage and soft cage. Langmuir 30:5739

Zylyftari G, Lee JW, Morris JF (2013) Salt effects on thermodynamic and rheological properties of hydrate forming emulsions. Chem Eng Sci 95:148

Zylyftari G, Ahuja A, Morris JF (2015) Modeling oilfield emulsions: comparison of cyclopentane hydrate and ice. Energy & Fuels 29:6286